Investigation of the Self-Calibration Function for IrO_X-based pH Sensors

Paul Marsh[1], Fatemeh Mohseni[1], J.-C. Chiao[3] and Hung Cao[1,2]
[1]Department of Electrical Engineering and Computer Science, University of California Irvine, Irvine, CA 92697, USA
[2]Department of Biomedical Engineering, University of California Irvine, Irvine, CA 92697, USA
[3]Department of Electrical and Computer Engineering, Southern Methodist University, TX 75205, USA
hungcao@uci.edu

***Abstract*—This paper explores a potential performance control strategy for the uses of a self-calibrating, remotely-accessible, electrodeposited iridium oxide-based (IrO_x) pH sensing system. Previous works have investigated deposition parameters, onboard thick film reference electrodes, and embedded applications for electrodeposited IrO_x pH sensors on flexible and biocompatible polyimide substrates as applied to passive wireless systems. As complete devices have been demonstrated, the logical next step is to investigate performance improvements. To that end, a self-calibration scheme is investigated herein to enhance longevity and performance, where potentiostatic control is used to return the thin film to a specific material state. This method can be coupled with the aforementioned passive wireless system, to be miniaturized and applied to a variety of applications. The method investigated provides design methodologies towards the ultimate goal of a long-term, self-calibrating IrO_x pH sensing system, operated and monitored remotely.**

Keywords—pH, iridium oxide, wireless, self-calibration

I. Introduction

The monitoring of pH aids greatly in the diagnosis of a multitude of human physiological, animal physiological, and environmental pathologies [2, 3]. Due to the importance of these sensors, a multitude of transducer and fabrication techniques and material types have been investigated over the last several decades [4]. Previously, we have demonstrated pH sensors based on electrodeposited iridium oxide (IrO_x) thin films, on various substrates, as well as entire sensing systems with wireless power transfer and signal transduction [1, 5, 6]. However, as in many pH sensing applications, one of the main difficulties of use is maintaining good performance via frequent calibrations [4]. This is one of the reasons that glass-encased dual-junction silver/silver-chloride (Ag/AgCl) probes have become ubiquitous: they feature relatively stable and invariable sensitivities. Owing to their surrounding saturated electrolytes, chlorine ion concentration is minimally altered over time; therefore, the reference electrode (RE) side of the probe maintains a steady offset (standard) potential while the working electrode (WE) side benefits from low drifts in sensitivity. When IrO_x WE or pseudo-RE electrodes are used, they face a similar issue but with heightened effects: their sensitivity and standard potential tend to drift over time while significant initial variance exists across a similarly-manufactured batch of devices; sensitivity could potentially vary as much as 10% [7].

The mechanisms underlying IrO_x pH sensing electrode performance degradation phenomena are complex but it is consistently suggested that some combination of oxygen presence within the thin film [8], pore wall and surface end group termination [9], ligand redox state [10, 11], and thin film mass loss due to potential cycling [12] contribute to changes in the thin film electrical responses. It was first suggested by Hitchman *et al.* [11] that, to an extent, potential responses to solution pH could be controlled by pre-conditioning electrodeposited IrO_x at a specific potential; in essence, the spatially-averaged redox state of the IrO_x ligands constituting the thin film were altered. As differing ratios of electron to proton production within the film, due to differing IrO_x ligands, have been theorized to account for "super-Nernstian" (>59 mV/pH) sensitivity [10], it stands to reason that alterations in spatially-averaged redox state (likely on the film surface) will affect potential responses. Carroll *et al.* [7] took this a step further by demonstrating that it was not necessary to perform this as pre-conditioning; instead, they found that a sufficiently long application of particular potentials at any time would produce electrodeposited IrO_x electrode batches which featured highly similar sensitivities and standard potentials.

Fundamentally, the work by Carroll *et al.* was the first demonstration of a self-calibrated IrO_x pH sensor. In the intervening years, there has been little expansion or integration of that work into more complex systems, despite the obvious benefit of well-controlled performance variation and the possibly significant extension of device lifetime. With a proper application of this technique, pH sensors can be returned to known calibration values (i.e. sensitivity values) multiple times over the course of their lifetime, making panel calibration redundant and prolonging operating terms. It is worth noting, however, that the demonstration by Carroll *et al* took place on Si substrates, in a rod form, as part of a flow-through cell. The effectiveness of this technique may vary with macro-scale surface morphology and flow

This work was supported by the National Science Foundation (NSF) CAREER Award #1917105 (H.C.); the GAANN fellowship from the US Dept. of Education (P.M.); and a setup fund (H.C.) and fellowship (F.M.) from the Henry Samueli School of Engineering at UC Irvine.

978-1-7281-6801-2/20/$31.00 ©2020 IEEE

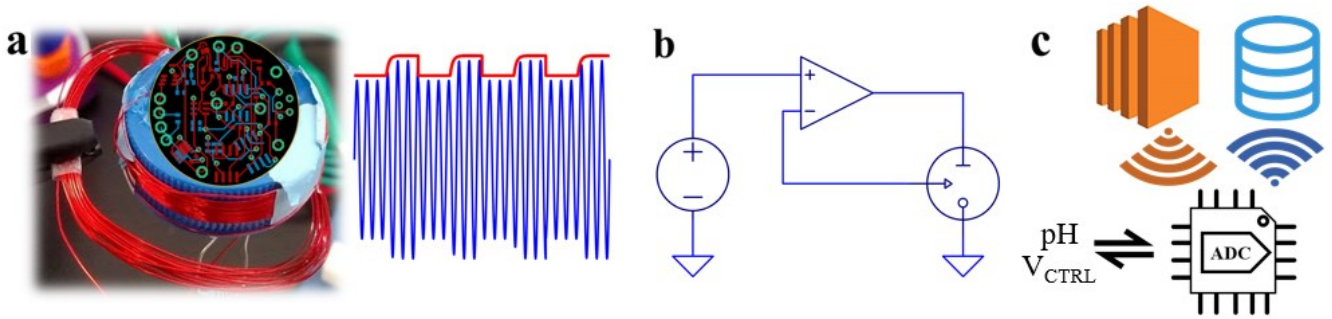

Fig. 1 Overview of an example complete system. (**a**) System includes a cap-integrated antenna and circuit for inductive power transfer and load-modulation signal transduction [1] (left hand panel). This circuit converts DC voltage resulting from the pH probe into a square wave voltage via an onboard voltage controlled oscillator (VCO); this VCO-generated square wave modulates the load of a receiving antenna through a parallel transistor, which manifests as a modulation in the transmitting antenna's amplitude envelope (right hand panel). This envelope modulation can be extracted and converted to a pulse count, which in turn relates to an as-designed voltage-to-frequency calibration. (**b**) Simple example of potentiostatic control circuit; DC supply indicates a control signal (V_{CTRL}). To accommodate the methods presented herein, the overall system will eventually require this circuitry onboard the cap system. (**c**) A microcontroller to communicate digitized signals to cloud data storage (pH), and voltage control signals (V_{CTRL}) for self-calibration. The overall system will eventually require this circuitry to be present on the transmitting antenna side.

conditions, due to variances in transport-controlled reaction kinetics and similar issues, so demonstration on other geometries and types of substrates holds value.

In this work, we explore extension of our previous application-specific prototypes [1] to include the valuable feature of potentiometric calibration control as demonstrated by Carroll *et al*. Specifically, we demonstrate the method as being effective with IrO_x sensing electrodes on polyimide substrates and constructed in the planar form factors as used with our previous wireless demonstrations [1, 5]. Data are presented which identify variances in the calibration control for the electrodeposited IrO_x pH sensors. Concurrent with ongoing hardware and data pipeline investigations which are outside the scope of this paper, the overview of the system is illustrated in **Fig. 1** to help readers to understand the overall goal. For reference, V_{CTRL} refers to the potentiostatic operation voltage.

II. Methods and Materials

As per previous demonstration of the signal transduction portion in [1], pH calibration curves were taken as the ratio of measured open-circuit potential (OCP) between IrO_x working electrodes (WE) and a Ag/AgCl reference electrodes (RE) saturated with 1 M NaCl. As reported previously, a unity-gain op-amp voltage follower was used prior to a dedicated data acquisition unit (USB-6001, *National Instruments, Austin, TX*). Data characterizing sensor performance was taken without wireless communication [1, 6].

Buffer panels were composed of Britton-Robinson (B-R) buffers [13]. B-R buffers lack chlorine ions and Ethylenediaminetetraacetic acid (EDTA), so as to limit IrO_x redox reactions and RE potential drifts. For simplicity, only three points were recorded to establish estimations of sensitivity and linearity. Reference measurements were made with a commercial dual-junction glass pH electrode. The substrates and geometries follow the ones in [1]. The electrodes were stored in DI water in enclosed sample containers between testing operations discussed herein.

Potentiostatic self-calibration operations were performed using commercial potentiostat CHI 760E (*CH Instruments, Austin, TX*). Per experiments in [7], the working electrodes were held at 200 mV versus Ag/AgCl for 180 seconds. Current was supplied by a Pt wire counter electrode (CHI115, *CH Instruments, Austin, TX*) immersed 5 mm in length into a 10x phosphate buffered saline (PBS) electrolyte. For degradation studies (**Figs. 2** and **3**), electrodes were inspected every other day via OCP, cyclic

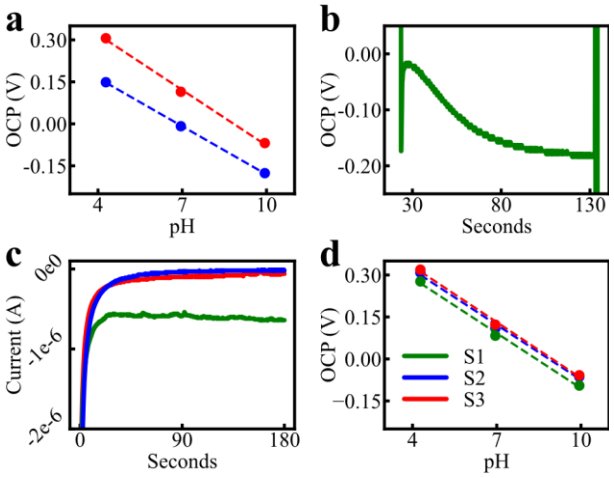

Fig. 2 Legend for all plots is inset in (**d**), bottom left corner. (**a**) Three-point calibration curves for samples 2 and 3, after eleven and sixteen days of use, respectively. Sensitivities are 57.4 and 66.1 mV/pH, respectively. Calibrations for both were performed on same day. (**b**) Extreme drift behavior presented in sample 1 at eleven days of use, with attempted calibration on same day as (**a**). (**c**) Potentiostatic operation on all three samples, after calibrations were conducted for (**a**) and (**b**). A 200-mV bias was applied in 10x PBS for 180 seconds. (**d**) Three-point calibration curves for all three samples, three days after the potentiostatic operation, as shown in (c). All samples show approximately 66 mV/pH sensitivities.

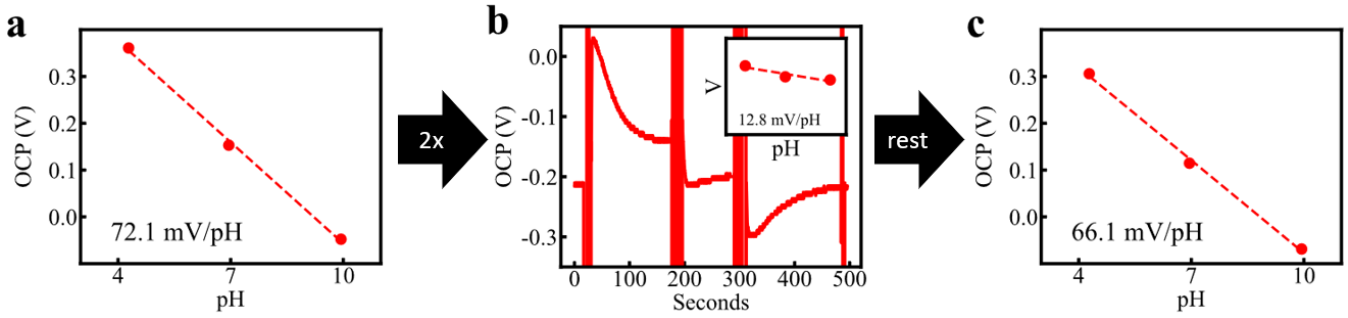

Fig. 3 Variable results with the potentiostatic operation. (**a**) Sample calibration on the day 13 of use. Sample underwent potentiostatic self-calibration operation twice following its sensitivity test. (**b**) Severe short-term drifts during calibration on the day 15 of use. Inset: estimated sensitivity with the drifts observed. (**c**) Calibration of the same sample on day 17 of use. No potentiostatic operation was performed between days 15 and 17; instead, the sample was placed at rest in DI water.

voltammetry (CV), and self calibration, all in 10x PBS, and three-point buffer panel calibration.

III. Results and Discussion

Results from a batch of three IrO_x electrodes are shown in **Fig. 2**. Some probes began to experience severe initial drift (~100 mV/min) after repeated uses. **Fig. 2(a)** shows two of those samples that were still operational after about 2 weeks of use, while **Fig. 2(b)** shows that the sample #1 had begun to experience a serious potential drift. Taken as an indication of Ir(III)/Ir(IV)/Ir(V) redox state changes, terminating group changes, or valency changes, this level of drift was used as a trigger indicator to apply the self-calibration operation. The current measured during the self-calibration operation, for all three samples, is shown in **Fig. 2(c)**. As can be seen, the sample #1 provided a low equilibrium exchange current density quickly, while the others would continue to draw oxidative currents for long periods. This phenomenon will be investigated further in the future to understand the nanoscale material changes. Regardless, the electrodes, after self-calibration, feature highly similar sensitivities and standard potentials across the batch, as shown in **Fig. 2(d)**, in keeping with data shown for the electrodes from similarly-constructed batches in [7].

Overall, the process did feature some inconsistencies which will require further investigation. **Fig. 3** demonstrates one such example. After 13 days of use, one sample underwent buffer calibration and potentiostatic self-calibration operation; afterwards, it showed serious drift and a lower sensitivity response. After resting the device in DI water for two days, a three-point calibration was conducted again; as shown in **Fig. 3(c)**, the sensitivity recovered. It is our experience that occasionally the samples responded to the treatment within different time windows, as some required time to rest while others returned to original performance parameters immediately. Although there might be potential inconsistencies in handling, storage, or connector attachment processes, the infrequent observations of a variable "rest time" associated with the self-calibration operation will be elucidated in further studies.

IV. Conclusions

This work presents a promising method and initial results towards IrO_x-based pH sensors with self-calibration capacity. This holds values in enabling the ultimate goal of a long-lasting, remotely operated pH sensing system. With previously demonstrated advantages for load-modulated wireless iridium oxide pH sensors, expanding upon the highly useful and simple planar and miniature form-factor, we demonstrate a self-calibration method with potentiostatic operation to remotely recover from standard potential drift and sensitivity loss. Future works will delve into optimization of the potentiostatic operation, investigations of surface processes, and consistency of the self-calibration process.

Acknowledgment

The authors wish to thank Prof. G.P. Li for the generous support of the Graduate Assistance in Areas of National Need (GAANN) grant. The authors also wish to thank the National Science Foundation for their substantial CAREER award funding.

References

[1] P. Marsh, Y. Zhuang, Z. Xu, L. Heine, and H. Cao, "Sample Tube pH Monitoring via Passive Powering and Communication," in *2019 IEEE SENSORS*, 2019, pp. 1-4.

[2] O. Korostynska, K. Arshak, E. Gill, and A. Arshak, "Materials and techniques for in vivo pH monitoring," *IEEE Sensors Journal,* vol. 8, pp. 20-28, 2007.

[3] P. Hinsinger, C. Plassard, C. Tang, and B. Jaillard, "Origins of root-mediated pH changes in the rhizosphere and their responses to environmental constraints: a review," *Plant and soil,* vol. 248, pp. 43-59, 2003.

[4] M. Ghoneim, A. Nguyen, N. Dereje, J. Huang, G. Moore, P. Murzynowski, *et al.*, "Recent Progress in Electrochemical pH-Sensing Materials and Configurations for Biomedical Applications," *Chemical reviews,* vol. 119, pp. 5248-5297, 2019.

[5] P. Marsh, M. Huerta, T. Le, X. Yang, J.-C. Chiao, and H. Cao, "Wireless Iridium Oxide-Based pH Sensing Systems," in *2018 IEEE SENSORS*, 2018, pp. 1-4.

[6] P. Marsh, W. Moore, M. Clucas, L. Huynh, K.-T. Kim, S. Yi, *et al.*, "Characterization of Flexible pH micro-Sensors Based on Electrodeposited IrOx Thin Film," in *IEEE Sensors*, Glasgow, Scotland, 2017.

[7] S. Carroll and R. P. Baldwin, "Self-calibrating microfabricated iridium oxide pH electrode array for remote monitoring," *Analytical chemistry,* vol. 82, pp. 878-885, 2010.

[8] J. Hendrikse, W. Olthuis, and P. Bergveld, "A method of reducing oxygen induced drift in iridium oxide pH sensors," *Sensors and Actuators B: Chemical,* vol. 53, pp. 97-103, 1998.

[9] Y. Ping, R. J. Nielsen, and W. A. Goddard III, "The reaction mechanism with free energy barriers at constant potentials for the oxygen evolution reaction at the IrO2 (110) surface," *Journal of the American Chemical Society,* vol. 139, pp. 149-155, 2017.

[10] P. VanHoudt, Z. Lewandowski, and B. Little, "Iridium oxide pH microelectrode," *Biotechnology and bioengineering,* vol. 40, pp. 601-608, 1992.

[11] M. L. Hitchman and S. Ramanathan, "Evaluation of iridium oxide electrodes formed by potential cycling as pH probes," *Analyst,* vol. 113, pp. 35-39, 1988.

[12] S. Cherevko, S. Geiger, O. Kasian, A. Mingers, and K. J. Mayrhofer, "Oxygen evolution activity and stability of iridium in acidic media. Part 2.–Electrochemically grown hydrous iridium oxide," *Journal of Electroanalytical Chemistry,* vol. 774, pp. 102-110, 2016.

[13] J. E. Reynolds III, M. Josowicz, P. Tyler, R. B. Vegh, and K. M. Solntsev, "Spectral and redox properties of the GFP synthetic chromophores as a function of pH in buffered media," *Chemical Communications,* vol. 49, pp. 7788-7790, 2013.